Non-perturbative tricritical exponents of trails. II. Exact enumerations on square and simple cubic lattices



1988 J. Phys. A: Math. Gen. 21 1043

(http://iopscience.iop.org/0305-4470/21/4/029)

J. Phys. A: Math. Gen. 21 (1988) 1043-1053. Printed in the UK

# Non-perturbative tricritical exponents of trails: II. Exact enumerations on square and simple cubic lattices

A Guha†, H A Lim‡ and Y Shapir

Department of Physics and Astronomy, University of Rochester, Rochester, NY 14627, USA

Received 4 September 1987

**Abstract.** We present exact enumerations of trails (self-intersecting but non-overlapping lattice walks) tabulated according to their length ($l$), number of intersection ($I$) and end-to-end distance for the square lattice (up to $l=21$, $I=7$) and for the simple cubic lattice (up to $l=15$, $I=5$). We introduce a fugacity for intersection to explore the transition to a collapsed phase through a novel tricritical point which is unaccessible by the renormalisation group approach. The existence of tricritical points in both lattices is manifested by the divergence of the specific heat. The values of the tricritical couplings and exponents are extracted by a DlogPadé analysis. We find for the three-dimensional lattice $\nu_t \simeq 0.48$ and $\gamma_t \simeq 0.43$ ($\nu_t \simeq 0.52$ and $\gamma_t \simeq 1.25$ for the square lattice).

## 1. Introduction and motivation

Trails are self-intersecting, yet self-avoiding, lattice walks. They may cross through an already visited site but cannot go on any bond more than once. Their configurations thus provide a non-trivial interpolation between two of the most important problems in statistical mechanics: the free random walk (RW) and the self-avoiding walk (SAW). Malakis [1] and Guttman [2] have investigated the long-distance properties of trails by exact enumerations. These results showed that trails share the scaling behaviour of SAW [1, 2]. In the language of critical phenomena [3], allowing for site self-intersections is an 'irrelevant' perturbation and the trail model belongs to the SAW universality class described by the O($n$) (or O($2n$)) spin model in the limit $n \to 0$. This result was confirmed by a renormalisation group analysis near $d=4$ [4]. This study was based on a Hamiltonian formulation for the trails generating a functional in terms of $n$ interacting ($n \to 0$) $XY$ spins. The continuum version of that Hamiltonian is

$$\mathscr{H}[\phi^{+\alpha}(x), \phi^{\alpha}(x)] = \int \mathrm{d}^d x \left[ \frac{t}{2} \sum_{\alpha} \phi^{+\alpha}(x)\phi^{\alpha}(x) + \frac{1}{2} \sum_{\alpha} \nabla\phi^{+\alpha}(x) \cdot \nabla\phi^{\alpha}(x) + g\left( \sum_{\alpha} \phi^{+\alpha}(x)\phi^{\alpha}(x) \right)^2 - u \sum_{\alpha} (\phi^{+\alpha}(x)\phi^{\alpha}(x))^2 + \dots \right]. \tag{1}$$

Higher-order terms are irrelevant and may be discarded. This theory may be viewed as a O($2n$) spin model with an additional term due to the intersections and which breaks the symmetry to O(2)$\otimes P_n$($P_n$ is the permutation group of $n$ objects). Field

† Present address: AT&T Bell Laboratories, 480 Red Hill Road, Middletown, NJ 07748, USA.
‡ Present address: Supercomputer Computations Research Institute, Tallahassee, FL 32306-4052, USA.

0305-4470/88/041043+11$02.50  

theories for generalised interacting walks in which the $O(2n)$ symmetry is unbroken were derived by Jasnow and Fisher [5]. The same Hamiltonian with negative $g$ and $u$ has attracted much attention because it describes the random $XY$ model (for a review, see [6]). In this case, it is known that the randomness (proportional to $g$) is irrelevant (the specific heat exponent of the pure $XY$ model is positive [7]). The question of whether a random fixed point exists for stronger randomness is as yet unanswered. Below we demonstrate the non-perturbative appearance of a closely related fixed point.

The number of intersections in the trail configurations may be controlled by adding a conjugate fugacity: we associate with each intersection a factor $f = e^{\theta}$ where $\theta = \beta\varepsilon$ and $\varepsilon$ is the chemical potential for the formation of crossing. In the limit $\theta \to -\infty$, the regular SAW model is recovered; $\theta = 0$ are the regular trails and for $\theta \to \infty$, we expect the compact configurations (with the maximal number of crossings) to dominate. The transition from one regime to the other is expected to be described by a tricritical point similar to the $\Theta$ point in polymers [3] which is driven in the SAW model by an unrestricted monomer–monomer attraction. In the continuum version, the effect of increasing the fugacity is to increase the absolute value of the (negative) ratio $|u/g|$. So the tricriticality in trails is crucially different from that of the $\Theta$ point which occurs in SAW ($u = 0$) when the renormalised vertex $g$ (renormalised osmotic pressure) vanishes and the $(\tilde{\phi}^2)^3$ term is controlling the behaviour near the upper critical dimension ($d_u = 3$) [3]. The trail configurations at their tricritical point are expected to be non-Gaussian ($\nu \neq \frac{1}{2}$) in 3D. However, no perturbative fixed point associated with this tricritical transition may be found by the RG approach and the $\varepsilon$ expansion. Instead, the RG result shows the SAW fixed point to remain the only stable fixed point and its basin of attraction includes all the quadrant $u > 0, g > 0$. Since a tricritical point is always expected between a swollen phase (analogous to a second-order critical point) and a collapsed one (the transition to which is first order in the magnetic terminology), an intriguing puzzle remains to be resolved.

In the first paper of this series [8] (herafter referred to as I), we have presented exact enumeration results on a triangular lattice in which the existence of a trail tricriticality was exhibited for the first time. In the present paper, we report results from exact enumerations on square and cubic lattices that unequivocally demonstrate the presence of such a tricritical point in two and three dimensions.

The paper is organised as follows: in § 2 we explain the enumeration and present extensive tables of coefficients (up to length $l = 21$ and $l = 15$ for the square and the cubic lattices respectively). In § 3, the specific heat computations are presented and the location of the tricritical point is found. Section 4 is devoted to the DlogPadé analysis which we use in order to calculate the approximate values of the scaling exponents at this tricritical point. Section 5 is devoted to a comparison of results on square and triangular (presented in I) latttices and to further conclusions and inferences.

## 2. Definitions and tabulation of the series

For each one of the lattices, we have enumerated two series:

(a) $c(l, I)$—the total number of trails of length $l$ (measured in units of lattice spacing) and $I$ intersections;

(b) $d(l, I) = \Sigma_r r^2 n(l, I, r)$ where $n(l, I, r)$ is the total number of trails with length $l$, $I$ intersections and end-to-end distance $r$ (in units of lattice spacing).

**Table 1.** The coefficients $c(l, I)$ for the square lattice.

| $l/I$ | $\frac{1}{4}c(l, I)$ | | | | | | | |
|---|---|---|---|---|---|---|---|---|
| | 0 | 1 | 2 | 3 | 4 | 5 | 6 | 7 |
| 1 | 1 | | | | | | | |
| 2 | 3 | | | | | | | |
| 3 | 9 | | | | | | | |
| 4 | 25 | 2 | | | | | | |
| 5 | 71 | 8 | | | | | | |
| 6 | 195 | 34 | | | | | | |
| 7 | 543 | 108 | 6 | | | | | |
| 8 | 1 479 | 368 | 28 | | | | | |
| 9 | 4 067 | 1 108 | 142 | | | | | |
| 10 | 11 025 | 3 476 | 490 | 32 | | | | |
| 11 | 30 073 | 10 256 | 1 832 | 112 | | | | |
| 12 | 81 233 | 30 760 | 6 034 | 704 | | | | |
| 13 | 220 375 | 89 404 | 19 838 | 2 512 | 168 | | | |
| 14 | 593 611 | 261 408 | 63 336 | 9 800 | 656 | | | |
| 15 | 1 604 149 | 750 432 | 197 284 | 34 496 | 3 548 | | | |
| 16 | 4 311 333 | 2 159 144 | 610 750 | 117 168 | 14 660 | 1 008 | | |
| 17 | 11 616 669 | 6 137 576 | 1 851 152 | 390 384 | 54 800 | 4 480 | | |
| 18 | 31 164 683 | 17 459 552 | 5 594 876 | 1 265 072 | 205 560 | 21 600 | 608 | |
| 19 | 83 779 155 | 49 246 860 | 16 652 694 | 4 033 296 | 714 140 | 90 080 | 4 768 | |
| 20 | 224 424 291 | 138 898 496 | 49 464 764 | 12 697 576 | 2 448 052 | 354 256 | 33 472 | |
| 21 | 602 201 507 | 389 333 868 | 145 236 226 | 39 376 848 | 8 158 268 | 1 283 168 | 140 336 | 6 400 |

Tables 1 and 2 present $c(l, I)$ and $d(l, I)$ respectively for the square lattice up to $l = 21$ and $I = 7$. Tables 3 and 4 present the same series for the cubic lattice up to $l = 15$ and $I = 5$.

Using the coefficients $c(l, I)$, we construct the series

$$U_l(\theta) = \sum_I c(l, I)\, \mathrm{e}^{I\theta}. \tag{2}$$

With this series and the coefficients $d(l, I)$, we generate the series for the average end-to-end distance squared:

$$\langle r_l^2(\theta)\rangle = \sum_I d(l, I)\, \mathrm{e}^{I\theta} / U_l(\theta). \tag{3}$$

## 3. Evaluation of the specific heat

Rapaport [9] first suggested (in his paper on the $\Theta$ point) to use the divergence of the specific heat in order to locate the tricritical point. In I we have improved the method by using a linear extrapolation to obtain a better estimate for the asymptotic value. We believe this method to be more accurate (although, as explained below, it is not as useful for the cubic lattices due to the oscillatory behaviour of the series). The

**Table 2.** The coefficients $d(l, I)$ for the square lattice.

| | $\frac{1}{4}d(l, I)$ | | | | | | | |
|---|---|---|---|---|---|---|---|---|
| $l/I$ | 0 | 1 | 2 | 3 | 4 | 5 | 6 | 7 |
| 1 | 1 | | | | | | | |
| 2 | 8 | | | | | | | |
| 3 | 41 | | | | | | | |
| 4 | 176 | | | | | | | |
| 5 | 679 | 8 | | | | | | |
| 6 | 2 452 | 72 | | | | | | |
| 7 | 8 447 | 428 | 6 | | | | | |
| 8 | 28 120 | 2 096 | 48 | | | | | |
| 9 | 91 147 | 9 076 | 382 | | | | | |
| 10 | 289 324 | 36 376 | 2 112 | 64 | | | | |
| 11 | 902 721 | 137 584 | 10 696 | 368 | | | | |
| 12 | 2 777 112 | 498 672 | 47 808 | 2 624 | | | | |
| 13 | 8 441 319 | 1 747 548 | 200 366 | 13 328 | 520 | | | |
| 14 | 25 398 500 | 5 960 600 | 792 264 | 65 600 | 2 720 | | | |
| 15 | 75 744 301 | 19 883 648 | 3 002 084 | 293 184 | 18 556 | | | |
| 16 | 224 156 984 | 65 103 472 | 10 987 072 | 1 235 520 | 92 064 | 3 712 | | |
| 17 | 658 855 781 | 209 810 184 | 39 086 656 | 4 972 464 | 439 888 | 19 840 | | |
| 18 | 1 924 932 324 | 667 001 240 | 135 769 448 | 19 208 512 | 1 952 208 | 129 408 | 1 216 | |
| 19 | 5 593 580 859 | 2 095 392 460 | 462 261 110 | 71 873 296 | 8 214 588 | 647 520 | 29 664 | |
| 20 | 16 175 728 584 | 6 514 417 216 | 1 546 710 112 | 261 680 128 | 33 134 016 | 3 072 064 | 169 600 | |
| 21 | 46 572 304 083 | 20 066 513 388 | 5 098 302 274 | 930 790 672 | 129 198 908 | 13 558 368 | 999 920 | 19 712 |

**Table 3.** The coefficients $c(l, I)$ for the simple cubic lattice.

| | $\frac{1}{6}c(l, I)$ | | | | | |
|---|---|---|---|---|---|---|
| $l/I$ | 0 | 1 | 2 | 3 | 4 | 5 |
| 1 | 1 | | | | | |
| 2 | 5 | | | | | |
| 3 | 25 | | | | | |
| 4 | 121 | 4 | | | | |
| 5 | 589 | 32 | | | | |
| 6 | 2 821 | 252 | | | | |
| 7 | 13 565 | 1 560 | 36 | | | |
| 8 | 64 661 | 9 568 | 424 | | | |
| 9 | 308 981 | 54 200 | 3 756 | | | |
| 10 | 1 468 313 | 304 296 | 28 204 | 688 | | |
| 11 | 6 989 025 | 1 646 976 | 189 272 | 7 968 | | |
| 12 | 33 140 457 | 8 846 760 | 1 210 068 | 80 168 | 704 | |
| 13 | 157 329 085 | 46 562 408 | 7 309 076 | 624 560 | 17 368 | |
| 14 | 744 818 613 | 243 535 400 | 43 202 968 | 4 599 072 | 215 488 | 528 |
| 15 | 3 529 191 009 | 1 257 654 960 | 246 915 152 | 30 675 504 | 2 059 336 | 27 808 |

**Table 4.** The coefficients $d(l, I)$ for the simple cubic lattice.

| | $\frac{1}{6}d(l, I)$ | | | | | |
|---|---|---|---|---|---|---|
| $l/I$ | 0 | 1 | 2 | 3 | 4 | 5 |
| 1 | 1 | | | | | |
| 2 | 12 | | | | | |
| 3 | 97 | | | | | |
| 4 | 672 | | | | | |
| 5 | 4 261 | 32 | | | | |
| 6 | 25 588 | 496 | | | | |
| 7 | 147 821 | 5 208 | 36 | | | |
| 8 | 830 576 | 44 480 | 672 | | | |
| 9 | 4 566 917 | 337 656 | 9 260 | | | |
| 10 | 24 692 980 | 2 364 400 | 96 064 | 896 | | |
| 11 | 131 682 825 | 15 641 408 | 866 392 | 17 184 | | |
| 12 | 694 386 864 | 99 095 520 | 6 984 416 | 227 200 | 1 408 | |
| 13 | 3 626 770 709 | 607 193 704 | 52 289 524 | 2 386 608 | 42 008 | |
| 14 | 18 790 632 772 | 3 621 647 024 | 368 873 520 | 21 791 488 | 623 552 | 2 112 |
| 15 | 96 675 376 705 | 21 132 370 416 | 2 488 974 096 | 180 777 264 | 7 451 336 | 68 512 |

specific heat is defined as follows:

$$h_l(\theta)=\frac{1}{l}\frac{\partial^2}{\partial\theta^2}\log U_l(\theta)=\langle I(\theta)^2\rangle-\langle I(\theta)\rangle^2 \tag{4}$$

namely it measures the relative fluctuations in the number of intersections. Since no other singular point is expected, the value of $\theta$ for which the $h_l(\theta)$ diverge is a clear signature of the tricritical point. The maxima of $h_l(\theta)$, denoted by $\theta_{\max}(l)$, do not fall on the same point but rather show a regular shift as function of $l$. The linear extrapolation method consists of looking at $\theta_{\max}(l)$ against $1/l$ and locating the intercept on the $\theta_{\max}(l)$ axis (or equivalently, locating the value of $\theta_{\max}(l)$ at $1/l=0$).

Figure 1($a$) exhibits the specific heat plots $h_l(\theta)$ for $l=11$-20. In figure 1($b$), $\theta_{\max}(l)$ is plotted against $1/l$. The strong oscillations do not allow for good linear extrapolation like that made in I for the triangular lattice. Based on this plot, we estimate $\theta_t^{\mathrm{sq}}\sim 1.4$-1.5.

Corresponding plots for the cubic lattice are presented in figure 2($a$) ($l=11$-15) and 2($b$). The tricritical point is estimated at $\theta_t^{\mathrm{c}}\sim 1.5$-1.8.

## 4. DlogPadé analysis

### *4.1. Definitions*

After locating the tricritical point $\theta_t$, we proceed to compute the critical exponents and the tricritical value of the growth constant $\mu_t$. The latter and the exponent $\gamma$ are defined through the asymptotic behaviour of the number of configurations. We anticipate the following behaviour as $l\to\infty$:

$$U_l(\theta)\to\Gamma(\theta)l^{\gamma(\theta)-1}\mu^l(\theta). \tag{5}$$

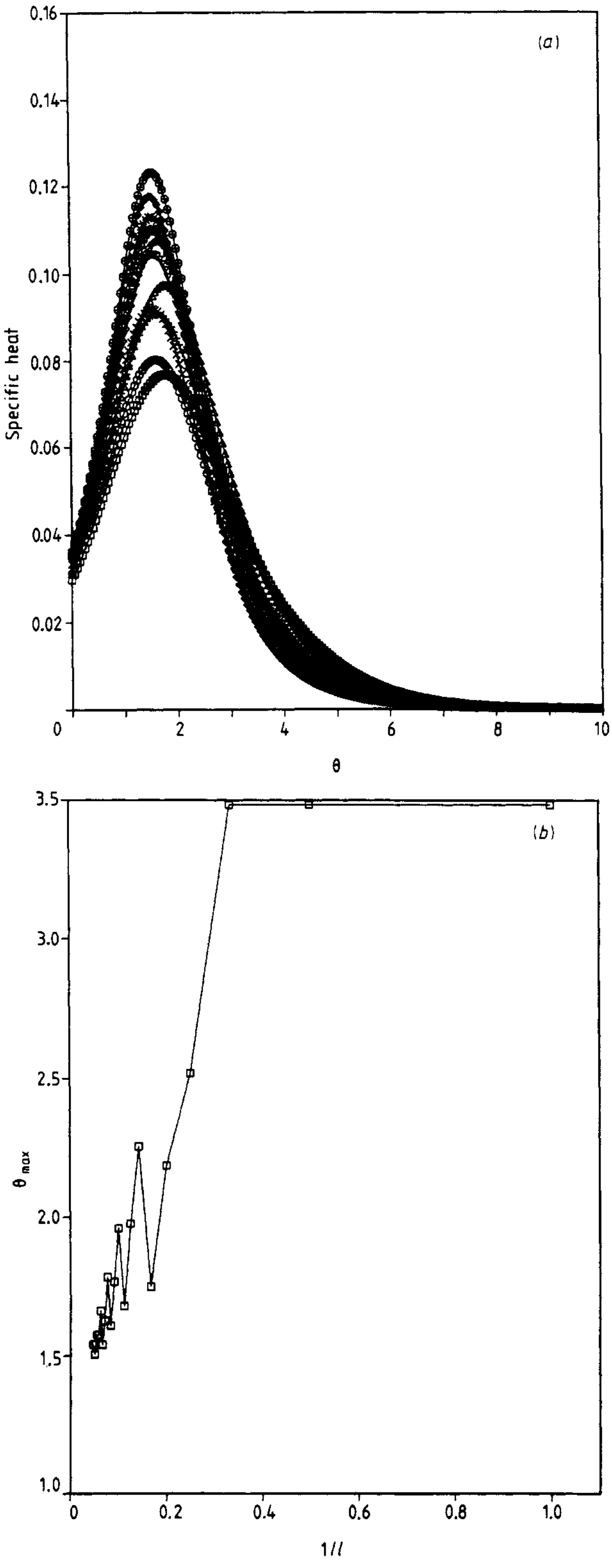


**Figure 1.** (*a*) Specific heat $h_1(\theta)$, $l = 11$–$21$ for the square lattice. (*b*) $h_1(\theta)$ against $1/l$ for the square lattice.

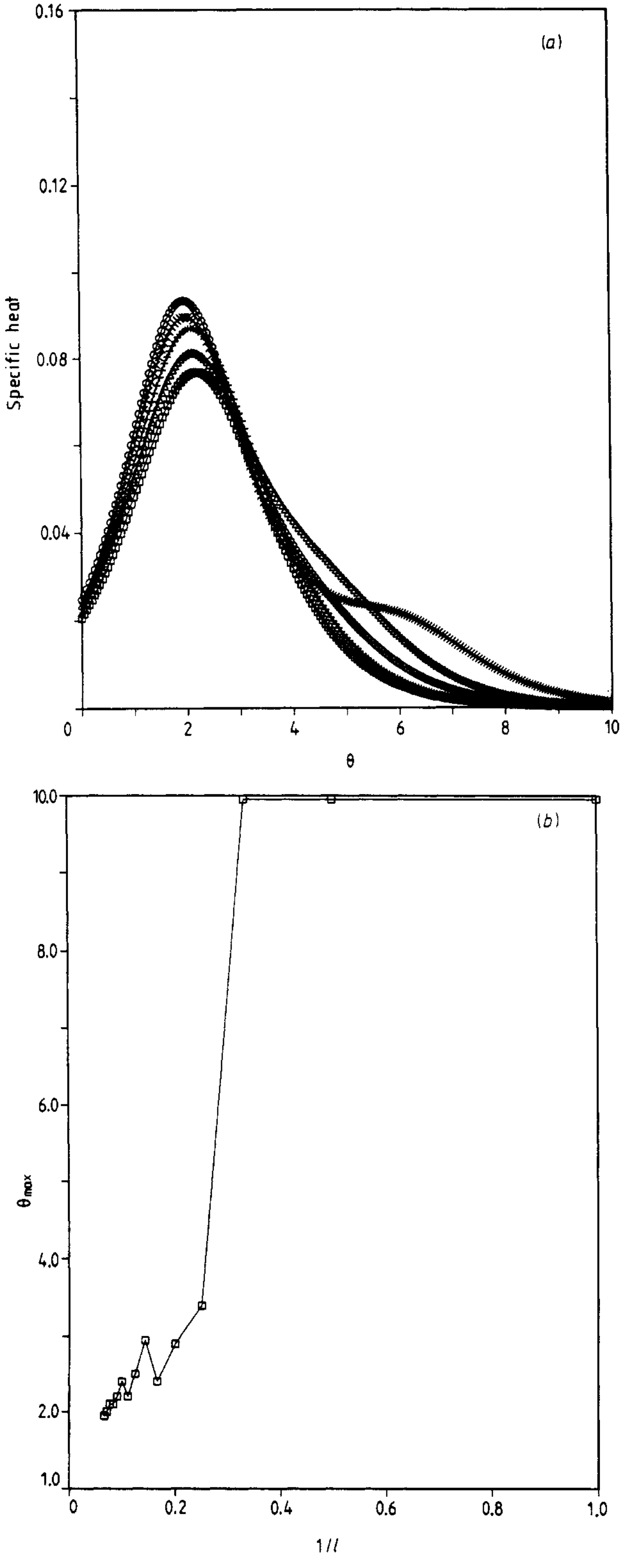


**Figure 2.** ($a$) Specific heat $h_l(\theta)$, $l = 11\text{-}15$ for the simple cubic lattice. ($b$) $h_l(\theta)$ against $1/l$ for the simple cubic lattice.

The amplitude $\Gamma(\theta)$ and the growth constant $\mu(\theta)$ are non-universal. For the exponent $\gamma(\theta)$, we expect a universal behaviour, namely that it will assume only one of the following three values: $\gamma(\theta)=\gamma_{SAW}$ for $\theta<\theta_t$, $\gamma(\theta)=\gamma_t$ at $\theta=\theta_t$ and $\gamma(\theta)=\gamma_c$ in the compact phase or $\theta>\theta_t$.

Similarly, the series for $\langle r_l^2(\theta)\rangle$ are expected to behave, as $l\to\infty$, like

$$\langle r_l^2(\theta)\rangle \to B(\theta) l^{2\nu(\theta)}. \tag{6}$$

$B(\theta)$ is non-universal but $\nu(\theta)$ is anticipated to assume one of the following three values: $\nu(\theta)=\nu_{SAW}$ for $\theta<\theta_t$, $\nu(\theta)=\nu_t$ for $\theta=\theta_t$ and $\nu(\theta)=(1/d)$ for $\theta>\theta_t$ (compact phase).

### 4.2. *Results for the square lattice*

The extrapolated value of $\theta_t^{sq}$ for the 2D square lattice is between 1.4 and 1.5. The last maxima $\theta_{max}(l=21)$ is at $\theta=1.55$. We present the result from the DlogPadé analysis for these values of $\theta$ in table 5.

**Table 5.** The exponents $\gamma_t^{sq}$ and the growth paramter $\mu_t^{sq}$ for different values of $\theta$ on the square lattice.

| | $\gamma_t(\mu_t)$ | | |
|---|---|---|---|
| $[L/M]/\theta$ | 1.4 | 1.5 | 1.55 |
| [8/9] | 1.229 (2.967) | 1.249 (3.070) | 1.234 (3.114) |
| [9/8] | 1.262 (3.010) | 1.250 (3.090) | 1.231 (3.128) |
| [9/9] | × (×) | 1.276 (2.935) | 1.260 (3.023) |
| [9/10] | 1.321 (3.051) | 1.267 (3.111) | 1.240 (3.142) |
| [10/9] | 1.273 (3.106) | 1.252 (3.145) | 1.232 (3.167) |
| [10/10] | 1.169 (3.142) | 1.181 (3.191) | 1.185 (3.213) |

The results for $\gamma_t$ and $\mu_t$ (in parentheses) are given for the highest possible diagonal, $[M/M]$, and off-diagonal, $[M-1/M]$ and $[M/M-1]$ approximants. Defective poles are denoted by crosses. We note immediately that the highest approximant [10/10] deviates relatively in its results from the rest. This is a consequence of a pair of conjugate complex poles close to the real axis between the origin and the physical pole. However, it may also be a signature of a crossover to a different behaviour at higher order (namely longer trails). We choose to base our estimate for $\gamma_t$ on the other approximants and predict

$$\gamma_t^{sq}=1.25\pm0.02 \tag{7}$$

$$\mu_t^{sq}=3.10\pm0.06. \tag{8}$$

(Comparison with the results from the triangular lattice is made in § 5.)

The series for $\langle r_l^2(\theta)\rangle$ becomes very erratic in the tricritical region for $\theta\geq1.4$. Almost all approximants give defective poles. Only two of them have a relatively reasonable behaviour: [9/8] yields $\nu=0.542$ (0.997), 0.5285 (0.996) and 0.521 (0.994) (the numbers in parentheses are the 'location' of critical point which should be at unity exactly) for $\theta=1.4$, 1.5 and 1.55 respectively. For the same values of $\theta$, [10/10] gives: 0.628 (0.988), 0.544 (0.992) and 0.488 (0.996). From these values we estimate roughly, for the square lattice,

$$\nu_t^{sq} = 0.525 \pm 0.025. \tag{9}$$

### 4.3. *Results for the cubic lattice*

The extrapolated $\theta_t^c$ for the cubic lattice is between 1.5 and 1.8 while the last maxima is at $\theta_{max}(l=15) \simeq 2.0$. We therefore give the results from the highest diagonal and off-diagonal approximant for value of $\theta$ between 1.5 and 2.0. In table 6, we present the figures for $\gamma_t$ ($\mu_t$). We note that there is a very nice convergence for the results of the highest approximants around $\theta = 1.8$. We therefore choose these as our best estimates with error bars roughly set by the values at $\theta = 1.7$ and 1.9 respectively. Our best estimates are

$$\gamma_t^c = 0.43 \pm 0.05 \tag{10}$$

$$\mu_t^c = 6.16 \pm 0.20. \tag{11}$$

In table 7, the result for $\gamma_t$ (and the critical value which is supposed to be precisely unity) are given for the same range of $\theta$ and same approximants (note that [7/7] is ill behaved). From the other approximants around $\theta = 1.8$, we predict

$$\nu_t^c = 0.48 \pm 0.02. \tag{12}$$

**Table 6.** The exponent $\gamma_t^c$ and the growth paramter $\mu_t^c$ in the vicinity of $\theta_t^c$ of the cubic lattice.

| | $\gamma_t(\mu_t)$ | | | | | |
|---|---|---|---|---|---|---|
| $[L/M]/\theta$ | 1.5 | 1.6 | 1.7 | 1.8 | 1.9 | 2.0 |
| [5/6] | 0.775 (5.612) | 0.738 (5.716) | 0.699 (5.832) | 0.659 (5.958) | 0.619 (6.100) | 0.576 (6.247) |
| [6/5] | 0.533 (5.774) | 0.468 (5.919) | 0.408 (6.076) | 0.354 (6.246) | 0.306 (6.429) | 0.265 (6.624) |
| [6/6] | 0.619 (5.718) | 0.556 (5.852) | 0.493 (6.001) | 0.434 (6.162) | 0.380 (6.338) | 0.331 (6.527) |
| [6/7] | 0.569 (5.749) | 0.518 (5.878) | 0.473 (6.017) | 0.431 (6.165) | 0.394 (6.323) | 0.360 (6.491) |
| [7/6] | 0.593 (5.735) | 0.532 (5.869) | 0.477 (6.013) | 0.431 (6.165) | 0.398 (6.319) | 0.393 (6.458) |
| [7/7] | 0.647 (5.700) | 0.568 (5.843) | 0.493 (5.998) | 0.434 (6.162) | 0.381 (6.336) | 0.337 (6.520) |

**Table 7.** The exponent $\nu_t^c$ (and the critical coupling $\bar{\mu}_t^c \equiv 1$) in the vicinity of $\theta_t^c$ for the simple cubic lattice.

| | $\nu_t(\bar{\mu}_t)$ | | | | | |
|---|---|---|---|---|---|---|
| $[L/M]/\theta$ | 1.5 | 1.6 | 1.7 | 1.8 | 1.9 | 2.0 |
| [5/6] | 0.476 (0.982) | 0.474 (0.979) | 0.472 (0.976) | 0.469 (0.972) | 0.466 (0.968) | 0.461 (0.965) |
| [6/5] | × (×) | × (×) | × (×) | × (×) | × (×) | × (×) |
| [6/6] | 0.497 (0.979) | 0.497 (0.976) | 0.497 (0.972) | 0.497 (0.968) | 0.496 (0.964) | 0.494 (0.960) |
| [6/7] | 0.491 (0.980) | 0.490 (0.977) | 0.488 (0.973) | 0.486 (0.970) | 0.483 (0.966) | 0.479 (0.962) |
| [7/6] | 0.489 (0.980) | × (×) | 0.484 (0.974) | 0.479 (0.970) | 0.474 (0.967) | 0.466 (0.964) |
| [7/7] | 0.439 (0.915) | 0.487 (0.977) | 0.400 (0.980) | 0.324 (0.983) | × (×) | × (×) |

## 5. Comparisons and conclusions

In the present paper, we have explored the tricritical behaviour of trails on the square and the cubic lattices. The location of these points are extracted from the sharp divergences in the specific heat.

Results for the tricritical exponents in 3D are derived here for the first time. Especially since no perturbative RG fixed point exists, it will be important to derive independently these exponents either from exact enumeration on other 3D lattices or even better, from large-scale Monte Carlo computations or from finite-size phenomenological scaling.

The results for $\gamma_t^c$ and $\nu_t^c$ imply for the exponent $\eta_t^c$:

$$\eta_t^c = 2 - \frac{\gamma_t^c}{\nu_t^c} = 1.10 \pm 0.15. \tag{13}$$

This is an unexpectedly large value (especially compared to the situation in 2D, see below) which implies a strong decay like $|r|^{-2.1}$ for the 'correlation' (sum of all trails with end-to-end distance $r$).

The results for the square lattice may be compared with that of triangular lattice derived in I. According to the universality hypothesis, critical exponents should be independent of the lattice structure (although doubts may be raised for the present case in which the fixed point is non-perturbative and therefore it is not possible to 'prove' universality even arbitrary close to 4D). For the triangular lattice, we found (see I) $\nu_t^{tr} = 0.52 \pm 0.01$ and $\gamma_t^{tr} = 1.18 \pm 0.02$. The agreement for $\nu_t$ is perfect between the square and the triangular results. For $\gamma_t$, on the other hand, the triangular result is consistently smaller and this discrepancy remains to be resolved by longer series, the aforementioned numerical methods, or exact results using conformal invariance [10]. The series on the square lattice are longer ($l = 21$) than those we used to derive the value of $\gamma_t$ on the triangular lattice ($l = 15$). However, this by no means implies that the former yield more reliable results: there are more intersections (for the same length) on the triangular lattice and therefore the maximal number of intersections is the same ($I = 7$) for both lattices. In addition, the closed-packed triangular lattice is known to yield more accurate results since it does not suffer from interference of other singularities which leads to oscillation like the ones reported here (figure 2(*b*)). So we regard the triangular result for $\gamma_t$ as more plausible. However, even this smallest value still implies $\eta_t < 0$ in 2D which is not physical (since the correlation can increase as function of distance only within the collapsed phase). So we anticipate the asymptotic value of $\gamma_t$ will approach its upper limit $2\nu_t \simeq 1.04$ when longer series are derived (note that $\eta = 0$ was argued to be the exact value at the $\Theta$ point [10]).

We hope all the remaining open questions will stimulate more research, using the various methods that have been applied to the investigation of the $\Theta$ point, to explore this non-perturbative tricritical point of trails.

## Acknowledgments

Fruitful discussions with M E Fisher, P G de Gennes, Y Oono and V Privman are gratefully acknowledged. This work was supported in part by funds from the Xerox Webster Research Center and from the University of Rochester. We are also thankful to the high-energy physics group of the Department of Physics and Astronomy at the University of Rochester for their kind assistance in computing.

## References

[1] Malakis A 1976 *J. Phys A: Math. Gen.* **9** 1283
[2] Guttmann A J 1985 *J. Phys. A: Math. Gen.* **18** 567, 575
[3] de Gennes P G 1979 *Scaling Concepts in Polymer Physics* (Ithaca, NY: Cornell University Press)
[4] Shapir Y and Oono Y 1984 *J. Phys. A: Math. Gen.* **17** L39
[5] Jasnow D and Fisher M E 1976 *Phys. Rev.* B **13** 1112
[6] Hertz J 1985 *Phys. Scr.* **10** 1
[7] Harris A B 1974 *J. Phys. C: Solid State Phys.* **7** 1671
[8] Lim H A, Guha A and Shapir Y 1988 *J. Phys. A: Math. Gen.* **21** 773
[9] Rapaport D C 1977 *J. Phys. A: Math. Gen.* **10** 637
[10] Duplantier B and Saleur H 1987 *Phys. Rev. Lett.* **59** 539